for the characterizations. The phase formation examinations were done with Bruker AXS D8 Advance model X-ray diffractometer (XRD), which run at 40 kV and 30 mA (Cu-Kα radiation) in a step-scan mode (0.02º/2θ). The morphology of particles and elemental analysis (EDX) of samples were investigated by a scanning electron microscope (SEM). Eventually, the photoluminescence (PL) studies including the excitation and emission spectra and fluorescence decay curves as well as lifetimes were analysed by a spectrofluorometer (Photon Technology International, QuantaMasterTM 30).

Results and Discussion

Thermal analysis

The thermal behaviours of $Y_{1.40}Sm_{0.10}Sc_{0.50}O_3$ and $Y_{1.40}Dy_{0.10}Sc_{0.50}O_3$ phosphors were determined in the range 50 to1400 ºC and the plots are given in Fig. 1. DTA/TG curves of $Y_{1.40}Sm_{0.10}Sc_{0.50}O_3$ in Fig. 1a consist of DTA/TG curves of pure Sm_2O_3[8] and a mass loss of 1.2 weight% observed between 50–475 °C was associated with the removal of water adsorbed by the material due to the foam-like morphology Sm(III) oxide. However, the Dy^{3+}-doped $Y_{1.40}Sc_{0.50}O_3$ composition does not show any mass loss or endo/exo-thermic reaction up to 1400 ºC (Fig. 1b).

X-ray diffraction (XRD) analysis

Firstly, a pre-heat treatment process was applied at 800 ºC for 6 h, then the heat treatment at 1000 ºC for 6 h was applied for single phase formation. After the sintering process, the XRD analyses were conducted for both samples. The Fig. 2 shows the comparative XRD patterns of $Y_{1.40}Sm_{0.10}Sc_{0.50}O_3$ and $Y_{1.40}Dy_{0.10}Sc_{0.50}O_3$ phsophors. The phosphor samples were clearly indexed by cubic phase of Y_2O_3 (JPCDS cards No.- 00-043-1036). In this case no evidence of the secondary phase was observed, the heat treatments were enough to get single phase of host crystal. Additionally, the diffraction peaks become sharper as the temperature is enough, as an effect of crystallinity enhancement and there was no evidence change in peak positions in spite of the doping of Sm^{3+} and Dy^{3+}ions. Furthermore, Y_2O_3 is indexed for all samples although the composition was $Y_{1.50}Sc_{0.50}O_3$, initially.Moreover, small amounts of Sm^{3+} and Dy^{3+}dopant ions have been incorporated into the host lattice and caused any distortions in the lattice structure or any secondary phase formations as it can be clearly seen in unaltered and similar diffraction patterns.The phosphors were well-crystallized in the cubic structure and the lattice parameters are a = b = c = 9.845 Å, α = 90°, β = 90° and γ = 90°.

SEM-EDX analysis

SEM images and EDX results of synthesized $Y_{1.40}Sm_{0.10}Sc_{0.50}O_3$ and $Y_{1.40}Dy_{0.10}Sc_{0.50}O_3$ phosphors are shown in Fig. 3 The particle size distibution measured directly from SEM images were approximately in the

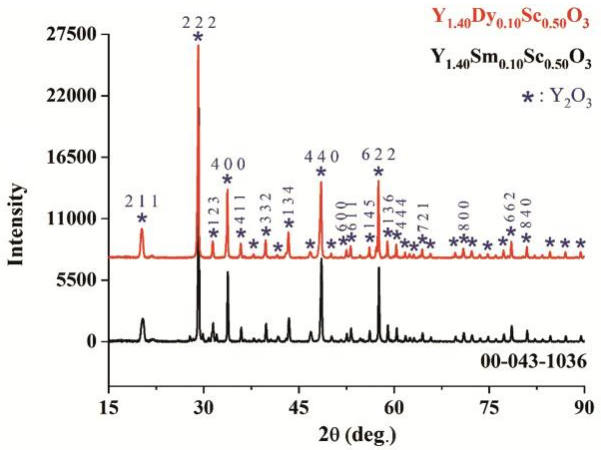

Fig. 2 — The comparative XRD patterns of $Y_{1.40}Sm_{0.10}Sc_{0.50}O_3$ and $Y_{1.40}Dy_{0.10}Sc_{0.50}O_3$

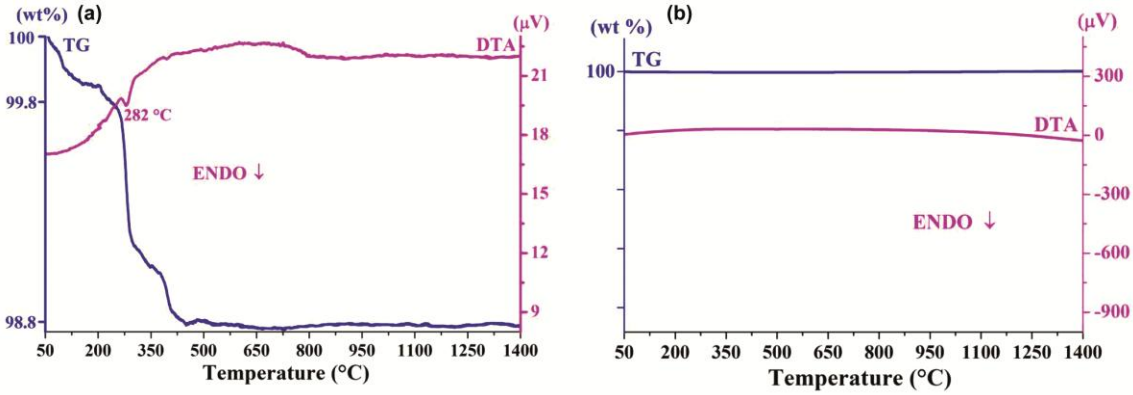

Fig. 1 — DTA/TG plots of (a) $Y_{1.40}Sm_{0.10}Sc_{0.50}O_3$ and $Y_{1.40}Dy_{0.10}Sc_{0.50}O_3$

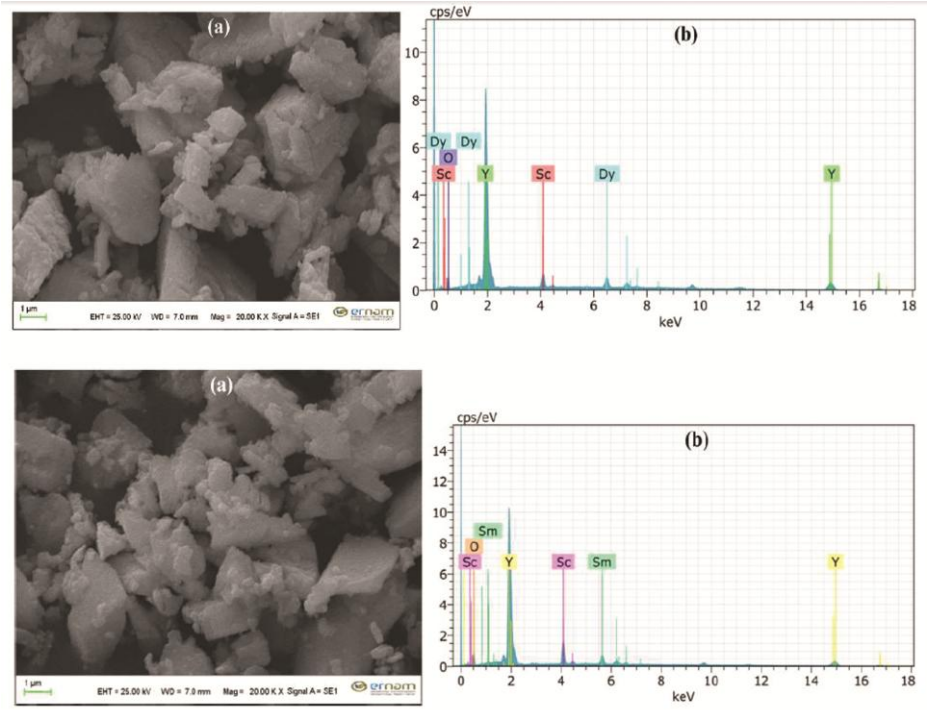

Fig. 3 — SEM images (a and b) and EDX plots (c and d) of $Y_{1.40}Sm_{0.10}Sc_{0.50}O_3$ (upper panel) and $Y_{1.40}Dy_{0.10}Sc_{0.50}O_3$ (lower panel) phosphor

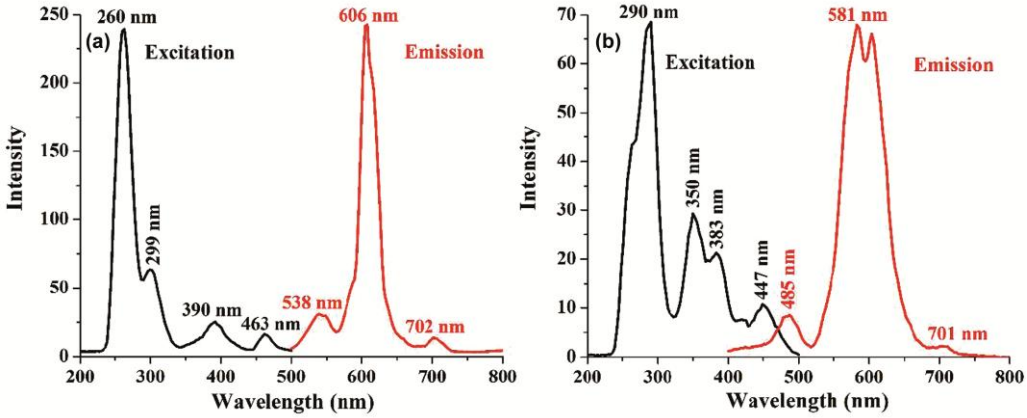

Fig. 4 — PL spectra of (a) $Y_{1.40}Sm_{0.10}Sc_{0.50}O_3$ and (b) $Y_{1.40}Dy_{0.10}Sc_{0.50}O_3$ phosphors

ranges of 0.27 – 0.70 µm and 0.25 –2.04 µm for $Y_{1.40}Sm_{0.10}Sc_{0.50}O_3$ and $Y_{1.40}Dy_{0.10}Sc_{0.50}O_3$ phosphors, respectively. The micron size particles of both samples have relatively irregular and agglomerated morphology, and composed of individual small particles with a rounded morphology. According to EDX results, the Sm and Dy element peaks had low intensities because their low quantities in compositions as expected.

Photoluminescence properties

The PL spectra of samples are given in Fig. 4. The excitation spectra of samples were recorded in the range of 200-500 nm using $\lambda_{emission}$= 606 nm for Sm^{3+}-doped and $\lambda_{emission}$ = 581 nm for Dy^{3+}-doped phosphor. Sm^{3+} has $4f^5$ configuration and complicated energy levels and diverse possible transitions between f-levels, so the transitions between f-levels are highly selective and have sharp line spectra. The excitation spectrum of $Y_{1.40}Sm_{0.10}Sc_{0.50}O_3$ which is shown in Fig. 4a has more than one peaks. The maximum excitation band in the range 260-290 nm are related with Sm^{3+}–O^{2-} charge transfer transitions[9]. The peaks at 390 nm and 463 nm are due to the excitation from ground-level $^6H_{5/2}$ to higher energy levels ($^6P_{7/2}$ and

Fig. 5 — Luminescence decay curves (a) by monitoring the $^4G_{5/2} \rightarrow {}^6H_{7/2}$ transition at ~606 nm in $Y_{1.40}Sm_{0.10}Sc_{0.50}O_3$ and (b) by monitoring the $^4F_{9/2} \rightarrow {}^6H_{13/2}$ transition at ~581 nm in $Y_{1.40}Dy_{0.10}Sc_{0.50}O_3$ phosphor

$^4F_{5/2}$+$^4I_{13/2}$) of Sm^{3+} ion [9-11]. The PL emission spectrum of Sm^{3+}-doped phosphor in red region consists of three peaks near 538 nm, 606 nm and 702 nm, which are assigned to the intra-4f-shell transitions from the excited level $^4G_{5/2}$ to ground levels $^6H_{5/2}$[(9-12)], $^6H_{7/2}$[(9-12)], $^6H_{11/2}$[(11-12)], respectively.

It is proved with various phosphors (hosts) in previous studies that the emission colour of the trivalent dysprosium, Dy^{3+} ($^4f_9$ configuration) photoluminescence is close to white. The excitation and emission spectra of $Y_{1.40}Dy_{0.10}Sc_{0.50}O_3$ phosphor which are shown in Fig. 4b, has the strongest excitation at 290 nm and assigned to $^6H_{15/2} \rightarrow {}^4K_{13/2}$ + $^4H_{13/2}$ transisitons of Dy^{3+}. The peak at 350 nm is attributed to the hypersensitive transition $^6H_{15/2} \rightarrow {}^4M_{15/2}$+$^6P_{7/2}$ and other bands with peaks at 383 nm and 447 nm are related with $^6H_{15/2} \rightarrow {}^4I_{13/2}$ and $^6H_{15/2} \rightarrow {}^4I_{15/2}$ transitions, respectively. The yellowish white light emission of this phosphor is composed of blue (485 nm) and yellow (581 nm) colour regions and recorded under excitation of 290 nm. These emissions correspond to the transisions from the $^4F_{9/2}$ excited state to the $^6H_{15/2}$ and $^6H_{13/2}$ (corresponds to the hypersensitive transition) ground states, respectively[4, 9, 14-15].

Luminescence decay curves of samples recorded at λ_{em} = 606 nm and λ_{em} = 581 nm are shown in Fig. 5. All the data for every sample are wellfitted with the following double exponential decay:

where, I_0 and I are the luminescence intensity at initial time and at time t, respectively, A_1 and A_2 are constants, τ_1 and τ_2 are the decay time for the exponential components, respectively. Results for fitted decay curve of samples are given in the inset of the respective fugures. The $\tau_{average}$ results show that Sm^{3+}-doped phosphor has longer lifetime of 552.785 μs than Dy^{3+}-doped one with $\tau_{average}$ = 10.319 μs.

Conclusions

The $Y_{1.40}Sm_{0.10}Sc_{0.50}O_3$ and $Y_{1.40}Dy_{0.10}Sc_{0.50}O_3$ phosphors were synthesized by solid-state reaction method under open atmosphere resulting single phase ($Y_{1.50}Sc_{0.50}O_3$) and completely indexed with Y_2O_3 host lattice. It can be said that the Sc^{3+}-ions are substituted in Y_2O_3 host lattice. XRD studies showed that $Y_{1.40}Sm_{0.10}Sc_{0.50}O_3$ and $Y_{1.40}Dy_{0.10}Sc_{0.50}O_3$ phosphors have cubic crystal structure with high crystallinity. The particle size distributions were measured as 0.27 μm–0.70 μm and 0.25 μm–2.04 μm for $Y_{1.40}Sm_{0.10}Sc_{0.50}O_3$ and $Y_{1.40}Dy_{0.10}Sc_{0.50}O_3$ phosphors, respectively. The excitation spectra of both phosphors are in the UV-region below 300 nm and this phenomenon also confirms that the Sm^{3+} and Dy^{3+} interactions with host lattice are very strong. Thus, we can say that the energy transfer occurs between Sm^{3+}/Dy^{3+}ions and the host crystal ($Y_{1.50}Sc_{0.50}O_3$). The emission bands of phosphors are also well compatible with the related dopant ions in phosphors. So, synthesized phosphors in this study could be considered as candidate for white-emitting devices.

Acknowledgement

The authors would like to thank Karamanoglu Mehmetbey University, Scientific Research Projects Commission (BAP, project number: 11-M-17), Republic of Turkey, for financial support. The authors are grateful to Prof. Dr. Adil Denizli from

Hacettepe University, Department of Chemistry and Biochromatography and Biodiagnostics Research Group for their kind help.

References

1 Öztürk E & Karacaoglu E, *J Therm Anal Calorim*, 131(2018) 2261.
2 Velazquez D Y M, Soto L A H, Ramirez Á de J M, Carmona-Téllez S, Garfias-Garcia E, Falcony C & Murillo A G, *Ceram Int*, 41 (2015) 8481.
3 Li X, Chen Y, Qian Q, Liu X, Xiao L & Chen Q, *J Lumin*, 132 (2012) 81.
4 Shivaramu N J, Nagabhushana K R, Lakshminarasappa B N & Singh F, *J Lumin*, 169 (2016) 627.
5 Uzun E, Öztürk E, Kalaycioglu Ozpozan N & Karacaoglu E, *J Lumin*, 173 (2016) 73.
6 Muresana L, Popovici E J, Imre-Lucacia F, Grecu R & Indrea E, *J Alloy Compd*, 483 (2009) 346.
7 Najar A, Omi H & Tawara T, *Nanoscale Res Lett*, 9(2014) Article 356.
8 Ruiz-Gómez M A, Gómez-Solís C, Zarazúa-Morín M E, Torres-Martínez L M, Juárez-Ramírez I, Sánchez-Martínez D & Figueroa-Torres M Z, *Ceram Int*, 40 (2014) 1893.
9 Li Y-C, Chang Y-H, Lin Y-F, Chang Y-S & Lin Y-J, *J Alloy Compd*, 439 (2007) 367.
10 Zhang F, Wang Y & Tao Y, *Mater Res Bull*, 48 (2013) 1952.
11 Naresh V & Buddhudu S, *J Lumin*, 147 (2014) 63.
12 Deng H, Zhao Z, Wang J, Hei Z, Li M, Noh H M, Jeong J H & Yu R, *J Solid State Chem*, 228 (2015) 110.
13 Krishn K M, Anoop G & Jayaraj M K, *J Electrochem Soc*,154 (2007) J310.
14 Babu P, Jang K H, Kim E S, Shi L & Seo H J, *J Korean Phys Soc*, 54 (2009) 1488.
15 Shen W Y, Pang M L, Lin J & Fang J, *J Electrochem Soc*, 152 (2005) H25.